

Multi-frequency Polarization Properties of Blazars

Svetlana G. Jorstad and Alan P. Marscher

*Institute for Astrophysical Research, Boston University, 725
Commonwealth Ave., Boston, MA 02215*

Jason A. Stevens and E. Ian Robson

*Astronomy Technology Centre, Royal Observatory, Blackford Hill,
Edinburgh EH9 3HJ, UK*

Matthew L. Lister

*Department of Physics, Purdue University, 1396 Physics Building, W.
Lafayette, IN 47907*

Alastair M. Stirling

*University of Manchester, Jodrell Bank Observatory, Macclesfield,
Cheshire, SK11 9DL, UK*

Paul S. Smith

Steward Observatory, University of Arizona, Tucson, AZ 85721

Timothy V. Cawthorne

*Center for Astrophysics, University of Central Lancashire, Preston,
PR1 2HE, UK*

José-Luis Gómez

*Instituto de Astrofísica de Andalucía, Apartado 3004, Granada 18080,
and IEEC/CSIC, Gran Capita 2-4, 08034 Barcelona, Spain*

Denise C. Gabuzda

Department of Physics, University College Cork, Cork, Ireland

Walter K. Gear

*Department of Physics and Astronomy, Cardiff University, P.O. Box
913, Cardiff CF2 3YB, Wales, UK*

Abstract. We have obtained total and polarized intensity images of 15 AGNs with the VLBA at 7 mm at 17 epochs, accompanied at many epochs by nearly simultaneous measurements of polarization at 1.35/0.85 mm and at optical wavelengths. Analysis of the data shows an obvious connection between the polarized emission at high frequencies and the most strongly polarized features in parsec-scale jets. The largest deviations between polarization parameters at different frequencies are detected when a new compact knot emerges from the core, and are likely caused by very short time-scale (<1 week) polarization variability during the events.

1. Introduction

Optically violent variable quasars and BL Lac objects form the most energetic class of active galactic nuclei (AGNs), blazars. Blazars have highly relativistic radio jets and display strong and variable linear polarization from radio through optical wavelengths. VLBI has now progressed to the point that one can image the radio jet in total and polarized flux with resolution of 0.1 mas (e.g. Marscher et al. 2002; Attridge 2001). This provides a unique opportunity to search for relations between the polarization variability at high frequencies and structural and polarization changes in VLBI maps that can establish connections between different emission regions in the source. Such observations are complicated by requirement of simultaneous measurements at different wavelengths. Gabuzda & Sitko (1994) and Gabuzda et al. (1996) analyzed nearly simultaneous optical and 6 cm VLBI polarization data of 8 blazars (BL Lac objects and the quasar 3C 279) and found that the optical polarization position angle is aligned with the radio polarization position angle either in the VLBI core or in the jet component nearest to the core. They noted that strong optical polarization in these sources is associated with the formation and emergence of new compact knots. Lister & Smith (2001) have observed 18 high and low optically polarized radio-loud quasars with the VLBA (*Very Long Baseline Array*) at 22 and 43 GHz and in the optical region. They found a strong correlation between the polarization level of the unresolved parsec-scale radio core at 43 GHz and the overall optical polarization of the source. This implies a co-spatial origin of the emission at these wavelengths. Therefore, investigation of the evolution of parsec scale jet structure combined with multi-frequency polarization variability is one of only a few ways to relate high-frequency emission with specific features in AGN jets.

We have obtained total and polarized intensity images of 15 AGNs with the VLBA at 7 mm at 17 epochs from 25/26 March 1998 to 14 April 2001. The VLBA observations are accompanied at many epochs by nearly simultaneous (within 2 weeks) measurements of polarization at 1.35/0.85 mm as well at optical wavelengths. In this paper we present results that show substantial connections between VLBI jet features and polarization properties from radio to optical frequencies.

2. Sample and Observations

We observed AGNs characterized by resolved structure on 43 GHz VLBI images (Marscher et al. 2002) and high degree of linear polarization at 350 GHz (Nartallo et al. 1998). The sample consists of 8 quasars (0420-014, 0528+134, 3C 279, 3C 273, 1510-089, 3C 345, CTA 102, and 3C 454.3), 5 BL Lac objects (3C 66A, OJ 287, 1803+784, 1823+568, and BL Lac), and 2 radio galaxies (3C 111 and 3C 120).

The VLBA observations were carried out at 43 GHz in both right and left circular polarization. The right-left phase difference was calibrated in the Astronomical Image Processing System (AIPS) using a scan of 3C 279, while instrumental polarization “D-terms” were determined via the method of Leppänen et al. (1995). The electric vector position angle (EVPA) calibration was obtained by different methods: comparison with quasi-simultaneous Very Large

Array (VLA) observations, a method based on the assumption that the D-terms change slowly with time (Gómez et al. 2002), and using EVPA-stable features in the images of the jets in 3C 279, OJ 287, and CTA 102. Sequences of images for all sources can be found on our web-site: <http://www.bu.edu/blazars>.

Observations at 1.35 and 0.85 mm were performed at the James Clerk Maxwell Telescope (JCMT) using SCUBA (Holland et al. 1999) and its polarimeter (Greaves et al. 2003). Flux calibration was achieved with observations of the planets or JCMT secondary calibrators. The instrumental polarization (of about 1%) was measured during each run by making observations of a compact planet, usually Uranus.

Optical observations were obtained using the Steward Observatory 1.5 m telescope located on Mt. Lemmon, Arizona. Polarization and photometric measurements were acquired with the Two-Holer Polarimeter/Photometer (Sitko et al. 1985). All polarization measurements were unfiltered ($\lambda_{eff} \sim 6000 - 7000 \text{ \AA}$), except 3C 273, where a Kron-Cousins R filter was used to avoid major emission-line features. Data reduction of the polarimetry followed the procedure described in Smith et al. (1992). The instrumental polarization was found to be $\leq 0.1\%$. Stars with known polarization (Schmidt et al. 1992) were observed during each run to calibrate the position angle of the measured polarization.

3. Relation between Polarization Properties and VLBI Structure

Comparison of direction of the linear polarization at sub-mm and optical wavelengths with the jet structure and EVPA of the VLBI core or brightest polarized jet feature suggests separation of the sample into four classes.

The first class is *extremely polarized blazars*, which includes 2 quasars, 3C 279 and 3C 345, and 3 BL Lac objects, 3C 66A, 1823+568, and BL Lac. In these sources a significant portion of the parsec scale jet is polarized higher than the noise level, with degree of polarization of the brightest polarized feature (core or knot nearest to the core) up to 15%, while the overall optical and sub-mm fractional polarization reaches 20-30% (Fig. 1, left panel). Such high linear polarization implies a well ordered magnetic field. Variations of the EVPAs at all frequencies do not deviate more than 30° from the direction of the innermost jet at nearly simultaneous epochs (Fig. 1, right panel; see also Stirling et al. 2003). A higher fractional polarization at optical wavelengths indicates that the higher frequency emission originates in a localized section of the 43 GHz emission region.

The second class is *polarized VLBI-core-dominated* sources. This class consists mostly of quasars (0420-014, 0528+134, PKS 1510-089, and 2230+114), although one BL Lac object, OJ 287, shows similar properties. In these sources the most prominent polarized feature of the jet at 43 GHz is the VLBI core. The polarization of the core is variable both in degree and direction and might be aligned, transverse or oblique to the innermost jet direction at different epochs. Nevertheless, the polarization at high frequencies strongly correlates with that of the VLBI core except during periods connected with the formation of a new disturbance later identified as a superluminal knot. In such cases, inconsistency between parameters at different frequencies results from very short time scales of variability ($\sim 1-2$ days) with frequency-dependent lags. For example, the frac-

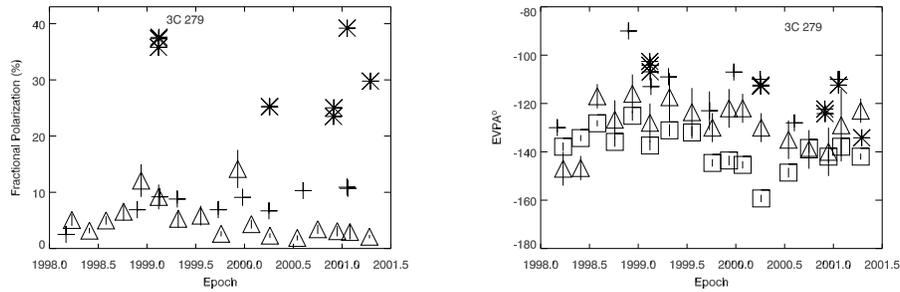


Figure 1. Variability of the fractional polarization (*left panel*) and EVPA (*right panel*) in the most polarized component near the core at 7 mm (triangles), at sub-mm (crosses) and optical (asterisk) wavelengths for the quasar 3C 279. Squares show position angle of the innermost jet.

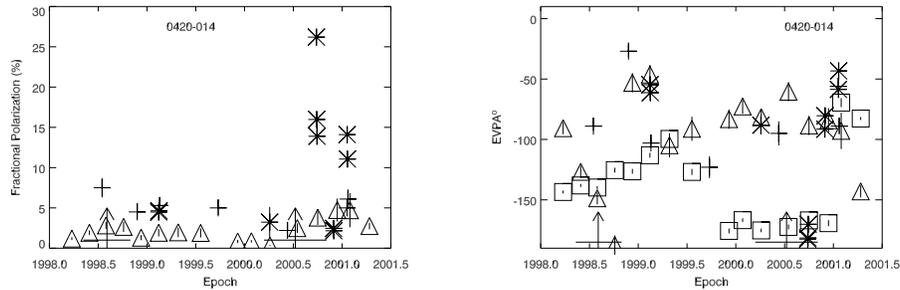


Figure 2. Variability of the fractional polarization (*left panel*) and EVPA (*right panel*) in the 7 mm VLBI core (triangles), at sub-mm (crosses) and optical (asterisk) wavelengths for the quasar 0420–014. Squares show position angle of the innermost jet. Arrows show time of ejection of superluminal knots.

tional optical polarization of the quasar 0420–014 changed from 26% to 14% within 3 days in September 2000 when a superluminal knot with apparent speed $7 \pm 3c$ (Jorstad et al. in preparation) was ejected (Fig. 2, left panel). These events are characterized by very strong rotation of the EVPA in the core (see Fig. 2, right panel) which is most likely caused by a change in opacity of the jet as the disturbance propagates through the core region.

The third class is *polarized VLBI-knot-dominated* AGNs. These sources, the 2 radio galaxies and the quasars 3C 273 and 3C 454.3, have unpolarized or very weakly polarized cores. The polarization at 43 GHz arises from a bright superluminal feature. The fractional polarization and EVPA of this feature are very similar to those in the sub-mm (see Fig. 3, left panel). This suggests that the VLBI core is intrinsically unpolarized, since Faraday effects are unlikely to be important at sub-mm wavelengths. However, the optical polarization appears to relate to that of neither a mm-bright knot nor the overall sub-mm polarization. This implies another origin of the polarized optical emission than is apparent in the radio jet.

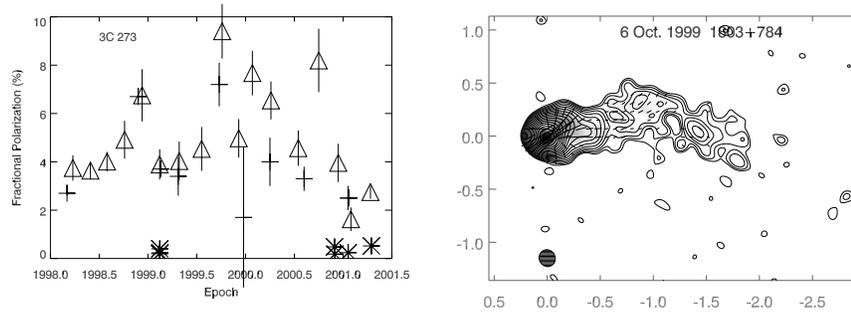


Figure 3. *Left panel:* Variability of the fractional polarization in the VLBI knot at 7 mm (triangles), at sub-mm (crosses) and optical (asterisk) wavelengths for the quasar 3C 273. *Right panel:* The 43 GHz total (contours) and polarized (grey scale) intensity image of the BL Lac object 1803+784. Sticks indicate direction of the electric vector.

The fourth class includes only one source, the BL Lac object 1803+784. The source has highly variable sub-mm polarization (from 1% to 11%). However, this is difficult to relate to mm polarization since the most polarized feature of the jet, the core, has fairly stable, circumferential polarization (see Fig. 3, right panel). This might imply the intrinsic toroidal magnetic field and a very small angle between the jet and line of sight.

Acknowledgments. This research was funded in part by US National Science Foundation grants AST-9802941 and AST-0098579.

References

- Attridge, J. M. 2001, *ApJ*, 553, L31
 Gabuzda, D. C., Sitko, M. L., & Smith, P. S. 1996, *AJ*, 112, 1877
 Gabuzda, D. C. & Sitko, M. L. 1994, *AJ*, 107, 884
 Gómez, J.-L. et al. 2002, VLBA Scientific Memo 30 (NRAO)
 Greaves, J. S., Holland, W.S., Jenness, T., et al. [13] 2003, *MNRAS*, 340, 353
 Holland, W. S., Robson, E.I., Gear, W.K. et al. [10] 1999, *MNRAS*, 303, 659
 Leppänen, K. J., Zensus, J. A., & Diamond, P. J. 1995, *AJ*, 110, 2479
 Lister, M. L. & Smith, P. S. 2000, *ApJ*, 541, 66
 Marscher, A. P., Jorstad, S.G., Mattox, J.R., & Wehrle, A.E. 2002, *ApJ*, 577, 85
 Nartallo, R., Gear, W.K., Murray A.G., Robson, E.I., & Hough, J.H. 1998, *MNRAS*, 297, 557
 Schmidt, G. D. 1992, *AJ*, 104, 1563
 Sitko, M. L., Schmidt, G. D., & Stein, W. A. 1985, *ApJS*, 59, 323
 Smith, P.S., Hall, P.B., Allen, R.G., & Sitko, M.L. 1992, *ApJ*, 400, 115
 Stirling, A. M., Cawthorne, T.V., Stevens, J.A., et al.[9] 2003, *MNRAS*, 341, 405